

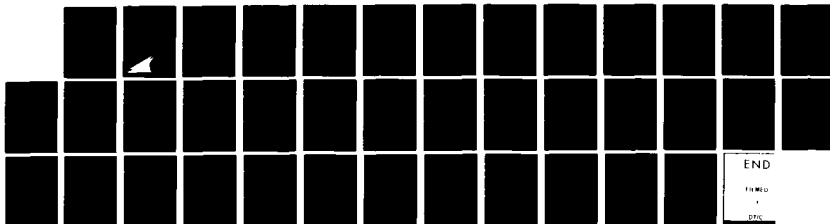
AD-A121 856

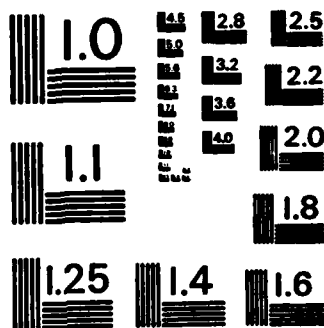
DEVELOPMENT OF AN AERODYNAMIC AND AEROELASTIC
PREDICTION CAPABILITY FOR C. (U) NIELSEN ENGINEERING
AND RESEARCH INC MOUNTAIN VIEW CA G D KERLICK ET AL.
SEP 82 NEAR-TR-277 N00019-81-C-0169 F/G 20/4

1/1

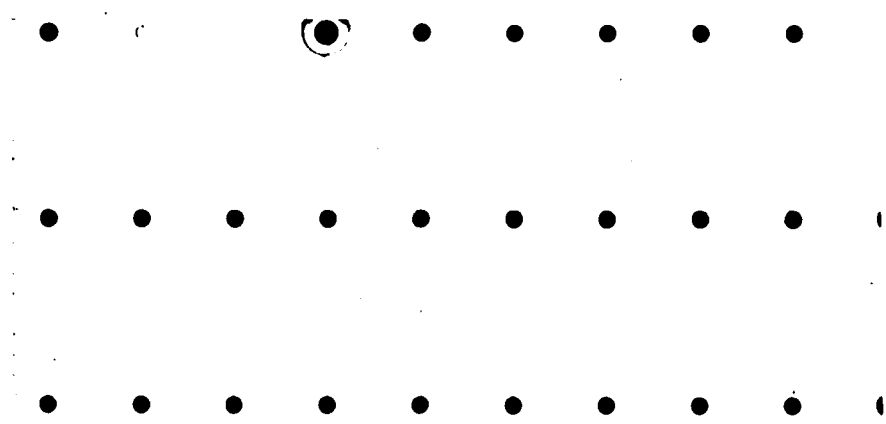
UNCLASSIFIED

NL



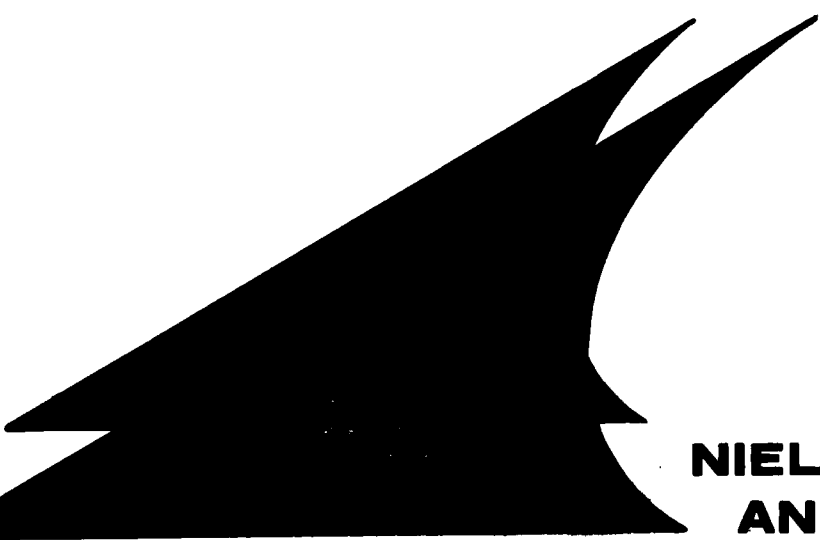


MICROCOPY RESOLUTION TEST CHART
NATIONAL BUREAU OF STANDARDS-1963-A



AD A 121856

FILE COPY



DTIC
ELECTIC
NOV 26 1982
E

APPROVED FOR PUBLIC RELEASE
DISTRIBUTION UNLIMITED

**NIELSEN ENGINEERING
AND RESEARCH, INC.**

82 11 26 030

OFFICES: 510 CLYDE AVENUE / MOUNTAIN VIEW, CALIFORNIA 94043 / TELEPHONE (415) 968-9457

DEVELOPMENT OF AN AERODYNAMIC AND
AEROELASTIC PREDICTION CAPABILITY
FOR CASCADES IN UNSTEADY
TRANSONIC FLOW

by

G. David Kerlick and David Nixon

NEAR TR 277

September 1982

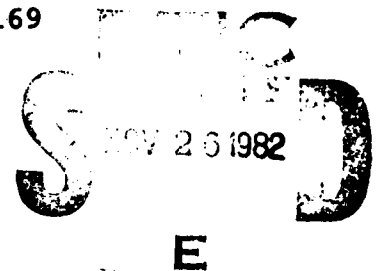
Prepared under Contract No. N00019-81-C-0169

for

NAVAL AIR SYSTEMS COMMAND
Washington, DC 20361

by

NIELSEN ENGINEERING & RESEARCH, INC.
510 Clyde Avenue, Mountain View, CA 94043
Telephone (415) 968-9457



APPROVED FOR PUBLIC RELEASE
DISTRIBUTION UNLIMITED

Unclassified

SECURITY CLASSIFICATION OF THIS PAGE (When Data Entered)

REPORT DOCUMENTATION PAGE		READ INSTRUCTIONS BEFORE COMPLETING FORM
1. REPORT NUMBER	2. GOVT ACCESSION NO. A121836	3. RECIPIENT'S CATALOG NUMBER
4. TITLE (and Subtitle) Development of an Aerodynamic and Aero-elastic Prediction Capability for Cascades in Unsteady Transonic Flow		5. TYPE OF REPORT & PERIOD COVERED Final Report
7. AUTHOR(s) G. David Kerlick and David Nixon		6. PERFORMING ORG. REPORT NUMBER NEAR TR 277
9. PERFORMING ORGANIZATION NAME AND ADDRESS Nielsen Engineering & Research, Inc. 510 Clyde Avenue Mountain View, CA 94043		8. CONTRACT OR GRANT NUMBER(s) N00019-81-C-0169
11. CONTROLLING OFFICE NAME AND ADDRESS Department of the Navy Naval Air Systems Command Washington, DC 20361		10. PROGRAM ELEMENT, PROJECT, TASK AREA & WORK UNIT NUMBERS
14. MONITORING AGENCY NAME & ADDRESS (if different from Controlling Office)		12. REPORT DATE September 1982
		13. NUMBER OF PAGES 36
		15. SECURITY CLASS. (of this report) Unclassified
		15a. DECLASSIFICATION DOWNGRADING SCHEDULE
16. DISTRIBUTION STATEMENT (of this Report) APPROVED FOR PUBLIC RELEASE DISTRIBUTION UNLIMITED		
17. DISTRIBUTION STATEMENT (of the abstract entered in Block 20, if different from Report)		
18. SUPPLEMENTARY NOTES		
19. KEY WORDS (Continue on reverse side if necessary and identify by block number)		
20. ABSTRACT (Continue on reverse side if necessary and identify by block number) A high-frequency version of the Ballhaus-Goorjian code LTRAN2 has been adapted to represent unsteady aerodynamic phenomena in transonic cascade flow. The modifications to the algorithm for high frequencies differ from those of Rizzetta and Chin in two ways: first, a second-order difference for the ϕ_{xt} term instead of a first order one is used, and second, a wake condition derived for the transonic small disturbance equation is applied. Then, in		

DD FORM 1 JAN 73 1473

Unclassified

SECURITY CLASSIFICATION OF THIS PAGE (When Data Entered)

Unclassified

SECURITY CLASSIFICATION OF THIS PAGE(When Data Entered)

Block 20 (concluded)

order to represent the cascade geometry, periodic boundary conditions and periodic tridiagonal solvers must be introduced. Examples of both oscillatory flows and indicial responses are presented. Application of the indicial method to unsteady cascades is discussed. Future work on the code will extend the applicability of the code to staggered, highly cambered cascades.

Accession For	
NTIS GRA&I	<input checked="" type="checkbox"/>
DTIC TAB	<input type="checkbox"/>
Unannounced	<input type="checkbox"/>
Justification	
By	
Distribution/	
Availability Codes	
and/or	
Dist	Special
A	



Unclassified

SECURITY CLASSIFICATION OF THIS PAGE(When Data Entered)

TABLE OF CONTENTS

<u>Section</u>	<u>Page No.</u>
1. INTRODUCTION	1
2. BASIC EQUATION	3
3. HIGH FREQUENCY CODE HTRAN2	4
3.1 Changes in the Algorithm	4
3.2 Changes to the Boundary Conditions	6
3.3 Wake Condition	6
4. MESH AND BOUNDARY CONDITIONS: STEADY CALCULATION	9
5. MESH AND BOUNDARY CONDITIONS: UNSTEADY CALCULATION	9
6. TEST RUNS OF THE CODE	10
6.1 Agreement Between Finite Difference and Indicial Calculation	11
7. HARMONIC ANALYSIS FOR FREE AIR AND CASCADES	11
8. CONCLUDING REMARKS	12
APPENDIX A NOTES ON THE COMPUTATIONS OF UNSTEADY TRANSONIC CASCADE FLOWS	15
APPENDIX B LOW STORAGE COMPUTATION OF THE ELEMENTARY SOLUTIONS	23
FIGURES 1 THROUGH 10	25
REFERENCES	35

1. INTRODUCTION

In jet engines, non-uniformities in the oncoming flow, caused perhaps by non-uniformities in the engine inlet, give rise to unsteady (possibly oscillatory) aerodynamic fluctuations, with the probability of structural-aerodynamic coupling in the compressor. This coupling can lead to flutter or other undesirable aeroelastic phenomena. It is highly desirable to be able to predict both the oscillatory aerodynamic forces and the structural-aerodynamic coupling in a compressor in order to find ways of alleviating or avoiding possible aeroelastic problems.

Because the flow through a real turbomachine is so complicated, various approximations have been developed which do not require inordinate amounts of computer time. A very common approximation consists of "unrolling" a blade row and treating it as an infinite two-dimensional cascade. If there are N identical blades, identically fixed in an axisymmetric rotor and equally spaced around the rotor circumference, then the cascade exhibits a fundamental periodicity every N blades. This is the fundamental periodicity of unsteady cascade flows. For steady flow through a rigid cascade, there are many instances where it is necessary to treat only the flow through a channel formed by two adjacent blades, that is, the fundamental periodicity of a steady cascade flow is one blade passage.

This problem is not so simple for an oscillating cascade. Although it is not difficult to formulate the elastic and inertial terms for the dynamic analysis of such a cascade, determining the unsteady aerodynamic loads is a truly formidable task, in view of the large number of different modes that are possible and the complicated nature of the aerodynamic coupling between blades. However, Lane (ref. 1) has been able to show that under certain circumstances there are only certain types of modes that can exist at flutter. If the blades are assumed

to be rigid, and the flow field equations can be linearized so that the principle of superposition is valid, then the only aeroelastic mode shapes that can exist - that is, the only eigenvectors that the system will have - involve the same contribution from the degrees of freedom of each blade, with each blade lagging (or leading) its neighbor by a constant phase. This means that the problem of determining the generalized aerodynamic forces for a cascade flutter analysis has been reduced to finding the forces for certain discrete modes - those involving a constant phase lag (or lead) from one blade to the next, with identical relative contributions from each blade mode.

If such a superposition principle holds in the transonic regime as well, then the transonic indicial method (refs. 2 and 3) can be applied. In this method, the essential nonlinearity of the solution, caused by the motion of the shock waves, is eliminated by means of a strained coordinate technique.

Finite difference calculations of the unsteady aerodynamic behavior of the cascade are therefore needed to calculate the response of the flow field to oscillatory and transient (stepwise, indicial) motions of the cascade, and to determine whether individual blade motions in the transonic regime can indeed be superimposed. The code described below will perform such finite difference calculations, provided that the cascade is unstaggered, of low camber, and composed of thin airfoils whose angle of attack or plunge amplitude undergoes small perturbations.

Although the main part of this report is concerned with the development of a computer code to treat the unsteady flow through cascades, some work has been done on the decoupling of the full cascade problem with variable interblade phase lag to the superposition of a number of elementary solutions that are independent of the phase lag. This analysis is given in Appendix A. Appendix B concerns a suggestion to reduce the computer storage necessary to calculate the elementary solution. Because of funding limits this idea was not implemented.

2. BASIC EQUATION

Computer codes for the simulation of unsteady transonic flows around isolated airfoils are in common use. These codes usually solve the transonic small disturbance (TSD) equation, since it may be solved consistently with a thin airfoil boundary condition. Full potential or Euler equation solvers require body fitted coordinate meshes, and for unsteady flows would require continual regeneration of the mesh.

We present here the first steps in a program to provide an unsteady analysis capability for transonic cascade flows, both by direct finite difference calculation and by the more economical perturbation theory. The simplest model problem for unsteady cascade flow is the unstaggered cascade of thin airfoils of low camber for which we can use the following form of the TSD equation (ref. 4):

$$\begin{aligned} A\phi_{tt} + 2B\phi_{xt} &= C\phi_{xx} + \phi_{yy} \\ A &= k^2 M_\infty^2 \delta^{-2/3} \\ B &= Ak^{-1} \\ C &= (1 - M_\infty^2) \delta^{-2/3} - (\gamma + 1) M_\infty^q \phi_x \end{aligned} \tag{1}$$

Here ϕ is the velocity potential, U_∞ and M_∞ are the free stream velocity and Mach number, respectively, γ is the adiabatic index, δ is the thickness parameter and q is the transonic scaling parameter. The quantities x , y , t , ϕ are in the scaled units of reference 4. The reduced frequency based on chord c is $k = \omega c / U_\infty$.

Ballhaus and Goorjian (ref. 4) solve Equation (1) in the case where $A = 0$, which applies for reduced frequencies less than about 0.2. The unsteady effects which we wish to study, primarily cascade flutter, occur at reduced frequencies (based

on blade chord) of about one to ten. Since LTRAN2 is not designed for these frequencies, high frequency modifications must be made.

Houwink and van der Vooren (ref. 5) and Hessenius and Goorjian (ref. 6), solve Equation (1), still with $A = 0$, but with improvements in the definition of C_p , and the airfoil and wake boundary conditions. Rizzetta and Chin (ref. 7) solve the full Equation (1) including the $A\phi_{tt}$ term, with improved boundary conditions, but report that they encounter stability problems. The modifications which we have made are described next.

3. HIGH FREQUENCY CODE HTRAN2

LTRAN2 has two components, a steady TSD equation solver by either successive line over-relaxation (SLOR) or approximate factorization (AF2) algorithms, and an unsteady solver based on the alternating direction implicit (ADI) algorithm. Only the unsteady solver is modified for high reduced frequencies. The airfoil boundary condition is applied on the split coordinate line at $y = 0$ (see Fig. 1).

3.1 Changes in the Algorithm

The high frequency modification requires two changes in the LTRAN2 algorithm. First, the ϕ_{tt} term is represented by a first order accurate three-point backward difference

$$\phi_{tt} = \frac{(\phi^{n+1} - 2\phi^n + \phi^{n-1})}{(\Delta t)^2} + \Delta t \phi_{ttt} + O(\Delta t^2) \quad (2)$$

This term requires the carrying of two extra levels of storage, and was also implemented by Rizzetta and Chin (ref. 7).

Another change is necessary for stability. In the original LTRAN2 algorithm, the first-order ϕ_{xt} difference has a leading truncation error $\Delta t \phi_{xtt}$. This is small compared to

$B\phi_{xt}$, but can be comparable to the $A\phi_{tt}$ term. Hence, we replace the first order difference in ϕ_t by a second order, three-point backward difference,

$$\phi_t = \frac{3\phi^{n+1} - 4\phi^n + \phi^{n-1}}{2\Delta t_1} + \frac{1}{3} (\Delta t)^2 \phi_{ttt} + O(\Delta t^3),$$

$$2\Delta t_1 \equiv 3t^{n+1} - 4t^n + t^{n-1}$$

We have found that this change in the algorithm leads to greatly enhanced stability.

The total algorithm is thus (compare ref. 4), x-sweep:

$$B(\Delta t_1)^{-1} \delta_x (3\tilde{\phi} - 4\phi^n + \phi^{n-1})_{j,k} = D_x f_{j,k} + \delta_{yy} \phi_{j,k}^n \quad (3)$$

y-sweep:

$$\begin{aligned} A(\Delta t)^{-2} (\phi^{n+1} - 2\phi^n + \phi^{n-1})_{j,k} + 3B(\Delta t_1)^{-1} (3\phi^{n+1} - 3\tilde{\phi})_{j,k} \\ = \frac{1}{2} \delta_{yy} (\phi^{n+1} - \phi^n)_{j,k} \end{aligned} \quad (4)$$

total:

$$\begin{aligned} \left[A(\Delta t)^{-2} + 3B(\Delta t_1)^{-1} - \frac{1}{2} \delta_{yy} \right] \phi_{j,k}^{n+1} \\ = D_x f_{j,k} + \frac{1}{2} \delta_{yy} \phi_{j,k}^n + B(\Delta t_1)^{-1} (4\phi^n - \phi^{n-1})_{j,k} \\ + A(\Delta t)^{-2} (2\phi^n - \phi^{n-1})_{j,k} \end{aligned} \quad (5)$$

The term $D_x f_{j,k}$ on the right hand side of Equation (3) of Reference 4 is the nonlinear term, including type-dependent differencing by means of a switching operator. This algorithm, like that of LTRAN2, is in conservation form.

3.2 Changes to the Boundary Conditions

Except for the wake condition, the changes to the boundary conditions are the same as those of reference 7, namely the definition of the pressure coefficient,

$$C_p = -2\delta^{2/3}(\phi_x + k\phi_t) \quad (6)$$

the airfoil tangency condition

$$\phi_y = f_x + k f_t \quad (7)$$

where $f(x,t)$ represents the airfoil surface, the downstream boundary condition

$$\phi_x + k\phi_t = 0 \quad (8)$$

and the initial condition

$$\phi_t(0) = h(x,y) \quad (9)$$

We take $h(x,y) = 0$. The mesh schematic for LTRAN2 and HTRAN2 appears in Figure 1.

3.3 Wake Condition

In order to derive the correct wake condition for the TSD Equation (1) we write it in divergence form

$$\begin{aligned} \frac{\partial}{\partial t} (A\phi_t + 2B\phi_x) - \frac{\partial}{\partial x} \left[(1 - M_\infty^2) \delta^{-2/3} \phi_x \right. \\ \left. - \frac{\gamma + 1}{2} M_\infty^2 \phi_x^2 \right] - \frac{\partial}{\partial y} (\phi_y) = 0 \end{aligned} \quad (10)$$

Let the wake be represented by the curve $y = f(x,t)$. Then the jump condition across the wake is given by

$$\left[A\phi_t + 2B\phi_x \right]_-^+ \frac{df}{dt} - \left[(1 - M_\infty^2) \delta^{-2/3} \phi_x - \frac{\gamma + 1}{2} M_\infty^q \phi_x^2 \right]_-^+ \frac{df}{dx} + [\phi_y]_-^+ = 0 \quad (11)$$

Here $[\]_-^+$ represents the jump between upper and lower surfaces. Requiring continuity of velocity normal to the wake implies

$$- \frac{df}{dx} [\phi_x]_-^+ \delta^{-2/3} + [\phi_y]_-^+ = 0 \quad (12)$$

Hence,

$$\left[A\phi_t + 2B\phi_x \right]_-^+ \frac{df}{dt} + \left[(M_\infty^2) \delta^{-2/3} \phi_x + \frac{\gamma + 1}{2} M_\infty^q \phi_x^2 \right]_-^+ \frac{df}{dx} = 0 \quad (13)$$

Dividing by $M_\infty^2 \delta^{-2/3}$, we obtain

$$\left[k k\phi_t + 2\phi_x \right]_-^+ f_t + \left[\phi_x + \frac{\gamma + 1}{2} \delta^{2/3} M_\infty^{q-2} \phi_x^2 \right]_-^+ f_x = 0 \quad (14)$$

which is a differential equation for $f(x,t)$. Continuity of pressure across the wake $[C_p]_-^+ = 0$ means

$$[\phi_x + k\phi_t]_-^+ = 0, \text{ or } \Gamma_x + k\Gamma_t = 0 \quad (15)$$

where

$$\Gamma = [\phi]_-^+, \quad \Gamma = \Gamma(kx - t)$$

thus we obtain from Equation (14) upon substitution of Equation (15):

$$kf_t + \left[1 + \frac{\gamma + 1}{2} \delta^{2/3} M_\infty^{q-2} (\phi_x^+ + \phi_x^-) \right] f_x = 0 \quad (16)$$

which is a partial differential equation for the wake surface $f(x,t)$.

Unfortunately, it is difficult to satisfy Equation (16) exactly, so we must look at various approximations for it.

The limiting case $\gamma \rightarrow -1$ (the Prandtl-Glauert theory) for Equation (16) is the linear wave equation $k f_t + f_x = 0$, with solution $f(x,t) = f(kx - t)$.

The low frequency limit $k \rightarrow 0$ of Equation (16) is merely $f_x \gg f_t$ and

$$f_x \approx 0, \quad \Gamma(x,t) = \Gamma(t) \quad (17)$$

as used by Ballhaus and Goorjian in LTRAN2.

In the high frequency limit we have $k f_t \gg f_x$ and $k \phi_t \gg \phi_x$. Unfortunately, the LTRAN2 mesh geometry does not permit a nonvanishing f_x . In order to be consistent with the TSD jump condition, Equation (14) we must have then for $f_x \approx 0$,

$$[k \phi_t + 2 \phi_x] f_t \approx 0 \quad (18)$$

which implies that the circulation propagates according to

$$\Gamma_x + \frac{k}{2} \Gamma_t = 0 \quad (19)$$

There is a small nonvanishing $[C_p]_-^+$ in this case, but numerical experiment shows it to be small, whereas violating Equation (14) by imposing Equation (15) and $f_x = 0$ causes the code to become unstable. For frequencies lower than $k = 0.2$, the original wake condition, Equation (17), is used. Although the ϕ_x term can be formally neglected in Equation (18) it is consistent to retain it in the present application since it is also retained in the basic equation, Equation (10).

4. MESH AND BOUNDARY CONDITIONS: STEADY CALCULATION

The steady solution for a cascade has all the blades at the same angle of attack. The solution is periodic, with a period of one blade spacing. Therefore, we solve the steady TSD equation for a single blade period, with periodic boundary conditions fore and aft, and airfoil boundary conditions for the blade surfaces at the top and bottom of the grid. This is illustrated in Figure 2. The mesh spacing in the x-direction is the same exponentially stretched mesh used in LTRAN2, but in the y-direction the mesh is clustered near the blade surfaces and symmetric about the line midway between adjacent blades. Note that the blades and wakes are represented by split coordinate lines aft of the leading edge gridpoint.

In developing the steady solution, two examples were run. For a NACA 0012 airfoil, solutions were calculated both for free air and periodic boundary conditions. At $M_\infty = .75$ we see the comparison in Figure 3. We could not obtain a converged solution for $M_\infty = .8$ and cascade boundary conditions. We expect that this is because the sonic line extends across the entire interblade spacing and that the code is exhibiting the same choking phenomena seen in real cascades, where the supersonic outflow does not permit enough mass to flow through the blade passage.

5. MESH AND BOUNDARY CONDITIONS: UNSTEADY CALCULATION

The unsteady solution is periodic over the whole cascade of N blades, so the unsteady calculation takes place on a mesh which is an N -fold replica of the steady-state mesh. Thus the entire cascade is represented, as can be seen in Figure 4. Again, the blades and wakes are represented by split coordinate lines.

First, the grid is swept in the y-direction from bottom to top with implicit quadridiagonal solvers used on the

y-constant lines. The interblade lines, the upper surfaces, and the lower surfaces are solved in turn, just as in LTRAN2.

Next the grid is swept in the x-direction. For the region ahead of the leading edge, periodic boundary conditions are used with a period of the entire grid (N interblade spaces), and the periodic tridiagonal solver is used. From the leading edge to trailing edge, each x-constant line for each interblade region is solved using a separate tridiagonal inversion with thin airfoil boundary conditions applied at both ends. Aft of the trailing edge, the periodic solver for the entire cascade (N blades) is used, with the upper surface potentials being obtained by adding the corrected circulation propagated back from the trailing edge according to the wake condition, Equation (19).

6. TEST RUNS OF THE CODE

The high frequency unsteady code equipped with periodic cascade boundary conditions will be called CHTRAN2. It can be applied to calculation of unsteady motions in either of two ways, just as LTRAN2 can. The code may be applied directly to calculate the oscillatory (flutter) motion of a cascade at a specified reduced frequency and interblade phase lag, or it may be used to calculate indicial responses in conjunction with the elementary solution of Appendix A, which are then inserted into convolution integrals (ref. 8) to determine the unsteady motion. The latter method has the advantage that a single calculation applies to a wide range of reduced frequencies and interblade phase angles.

The indicial response calculated here is for a 0.25 degree step change in angle of attack for blade #3 in a cascade of $N = 5$ blades, with all other blades remaining fixed. That is, the elementary solution of Appendix A. The airfoil shape is an uncambered NACA 0012, and the spacing between blades is one chord length. The free stream Mach number is 0.75. The

indicial function for lift coefficient for the moving blade is illustrated in Figure 5. The expected time delays for the neighboring blades are present in their indicial functions, not illustrated here.

6.1 Agreement Between Finite Difference and Indicial Calculation

Both finite difference (CHTRAN2) and indicial calculation (program CONVOL, ref. 9) which evaluates Duhamel's integral (ref. 8) were run for a five-blade cascade oscillating with all blades in phase. Figure 6 shows a low frequency case, $k = 0.2$, that shows almost exact agreement in the finite difference and convolution calculations of unsteady lift. Figure 7 shows a high frequency case. Here, the higher harmonics found in the finite difference schemes are not reproduced by CONVOL. In general, CONVOL will only produce those harmonics which are present in the forcing function.

7. HARMONIC ANALYSIS FOR FREE AIR AND CASCADES

Runs were made of CHTRAN2 in the case of an unstaggered, six-blade cascade of NACA 0012 airfoils with relative phase difference of 180° between the blades. Both torsional and bending modes were run at Mach numbers of 0.5 (to compare with Verdon and Caspar, ref. 10) and Mach 0.75 (to illustrate the transonic effects). A calculation using HTRAN2 for an isolated airfoil oscillating in angle of attack at Mach 0.80 was also run, to compare the unsteady transonic forces on an isolated airfoil with the cascade example at Mach 0.75 (the difference in Mach number is taken so that the sonic regions in each case are similar). The bending mode is illustrated in Figure 8 and the torsional mode in Figure 9.

Bending Mode - Figure 8 shows the real and imaginary parts of the first harmonic of the unsteady pressures for the fourth cycle of oscillation in airfoil plunge, of amplitude

$z_1 = .005$ chords, which corresponds to the blade bending mode. The phase difference between adjacent blades is 180° . The subsonic results show the same behavior as those of Verdon and Caspar (ref. 10), plotted in their Fig. 8, p. 47. The transonic case shows a phase change occurring in the region near the shock. Similar behavior was observed in a calculation for an isolated airfoil at $M_\infty = 0.8$.

Torsional Mode - Figure 9 shows the results of our calculation of the real and imaginary unsteady pressure coefficients for an oscillation of amplitude 1.0° in angle-of-attack, which corresponds to the blade torsion mode. The subsonic case compares in shape with Verdon and Caspar (ref. 10, Fig. 9, p. 48). Here again, the transonic case compares with the isolated airfoil at $M_\infty = 0.8$.

8. CONCLUDING REMARKS

In its present stage of development, the code CHTRAN2 can simulate by finite differences the unsteady transonic flow through an unstaggered cascade of up to 12 thin airfoils of low camber, such as might be found in a compressor, with arbitrary motion of each blade. The next step will be to allow for staggering of the blades. At that point it should be possible to compare the numerical calculation with experiment. For turbine flows with a large turning angle, it will be necessary to rederive the small disturbance theory for perturbations about a steady turning flow.

For cascades of more than about 20 blades, the storage on the CDC-7600 computer is inadequate. But even for fewer blades, it will be worthwhile to investigate the extent to which the behavior of the full flow field can be reconstructed from the solution for a single blade passage. If this can be done, the indicial method would be of even greater value.

Further tests of the indicial method are planned. It should be borne in mind that the indicial method is independent

of the particular finite difference code used. Thus, when full potential solvers for the cascade problem become available, the indicial method should be applicable.

APPENDIX A

NOTES ON THE COMPUTATIONS OF UNSTEADY TRANSONIC CASCADE FLOWS

In an oscillating cascade there is by definition a fundamental periodicity that occurs every $2N$ blades ($2N$ is the number of blades in the compressor row). The unsteady flow at each blade will have a periodic boundary condition, as in steady flow, but will lag by a phase angle of $(p/N)\pi$ in relation to the neighboring blade, where p is an integer less than or equal to N whose value is determined as part of the flutter solution. In a nonlinear transonic numerical scheme the choice is between computing the entire $2N$ blade sequence with the usual periodic boundary conditions at the extremities, or to compute the usual three blade cascade problem for each specified value of p . These numerical calculations are computationally expensive and it is desirable to reduce the overall cost of a flutter calculation. Both of these choices involve a large amount of computer time for practical cases, and in case of the first choice, a major development of a computer code. However, it is possible to devise a simpler approach to the problem.

The basic idea of this paper is to devise an elementary problem in which only one blade is in motion, the others being fixed; the motion may be any general time dependent function. This removes the problem of computing the flow for each blade phase angle. This elementary problem is solved for a particular moving blade and the functional form of the velocity potential for both space and time is then known. Because of periodicity in both space and time these elementary solutions can be superimposed, with reparameterized space and time variables, so that the sum of the solutions satisfies both the basic differential equation and the correct boundary conditions on every blade. Although the most important application of this superposition

principle is the development of the correct linearization of the transonic flow equations with discontinuities, these equations are much too complicated for an illustration of the superposition technique. Hence, in the following only a simple, subsonic problem is examined. The general theory is directly extendable to discontinuous transonic flows using the strained coordinate theory of Nixon (ref. 2).

ANALYSIS

Consider the cascade of $2N$ blades pictured in Figure 10 where blade $J+N$ and blade $J-N$ are identified. The equation for the perturbation velocity potential, $\phi(\bar{x}, t)$, due to a time-dependent behavior of the blades, will be linear and can be represented as follows:

$$L(\bar{x}, t)\phi = 0 \quad (A1)$$

Here, \bar{x} is a general vector coordinate centered on the blade of interest, t is time, and $L(\bar{x}, t)$ is a differential operator with variable coefficients. These coefficients arise from the mean steady flow solution about which the flow is perturbed, are functions only of \bar{x} , and are periodic in space with period of $2N$ blades. The time t only occurs through the inclusion of time derivatives. Such an operator occurs in the subsonic flow analysis of Verdon and Caspar (ref. 10) who use the equation

$$\left\{ \left(\frac{\partial}{\partial t} + \nabla\phi \cdot \nabla \right) \left(\frac{\partial}{\partial t} + \nabla\phi \cdot \nabla \right) + (\gamma - 1)\nabla\phi \left(\frac{\partial}{\partial t} + \nabla\phi \cdot \nabla \right) + \left[\frac{\nabla\phi \cdot \nabla\phi}{2} \right] \cdot \nabla - a^2 \nabla^2 \right\} \phi = 0$$

where ϕ is the steady state potential. For a staggered cascade the upstream and downstream boundary conditions will depend on the particular region of the flow that is being considered,

for example the far upstream boundary D_{Uj} and the far downstream boundary D_{Dj} shown in Figure 10. The boundary conditions will depend on the steady far field velocity, which has spatial periodicity and on the phase of the waves produced by the oscillating cascade. Since the individual blade flows are identical except for phase lag of jt_0 , it follows that the far field boundary conditions are

$$\begin{aligned}\phi_U(\bar{x}_U, t) &= g_U(\bar{x}_U, t_j) & \text{on } D_{Uj}, & \quad j = -N, N \\ \phi_D(\bar{x}_D, t) &= g_D(\bar{x}_D, t_j) & \text{on } D_{Dj}, & \quad j = -N, N\end{aligned}\tag{A2}$$

where \bar{x}_U , \bar{x}_D denote the location of the upstream and downstream boundaries, respectively, and g_U and g_D are the corresponding spatially asymptotic values of $\phi(\bar{x}, t)$. The time t_j is given by $t_j = t - jt_0$ where t_0 is the interblade phase lag. The tangential boundary conditions are

$$v_j(\pm\bar{x}, t) = f_j(\pm\bar{x}, t_j) \quad \text{on } S_j; \quad j = -N, N \tag{A3}$$

where v_j is the normal velocity component, f_j is a function of the specified perturbation of blade geometry and S_j denotes the location of the j th blade surface. The \pm signs denote conditions on the upper and lower surface of the blades, respectively. The effect of the interblade phase lag is seen in Equations (A2) and (A3) where the potentials ϕ_U , ϕ_D or the velocity of the j th blade at time t are given in terms of a function at a time t_j . For blade number 0, periodicity can be applied on $j = \pm N$. In addition to the above boundary conditions the wake condition is

$$\Delta C_p(\bar{x}, t) = 0 \text{ on } w_j$$

where ΔC_p is the pressure jump across the wake of the j th blade, w_j , and is a function of $\phi(\bar{x}, t)$. Now if the principle of superposition holds then a variable $\phi_j(\bar{x}_j, t)$ can be introduced such that

$$\phi(\bar{x}, t) = \sum_{j=-N}^N \phi_j(\bar{x}_j, t) \quad (A5)$$

where

$$\bar{x}_j = \bar{x} - \tilde{x}_j$$

and \tilde{x}_j is the location of the general coordinate system centered on the j th blade and $x_0 \equiv \bar{x}$. Assume that ϕ_j is such that

$$L(\bar{x}, t) \phi_j = 0 \quad (A6)$$

It is obvious that if Equation (A6) is used with Equation (A5) then Equation (A1) is recovered.

The operator $L(\bar{x}, t)$ is a differential operator with coefficients that are functions of the steady flow over a cascade and hence $L(\bar{x}, t)$ is periodic in the spatial dimensions. Thus $L(\bar{x}, t)$ is the same no matter on which blade the coordinate system is centered. Hence

$$L(\bar{x}, t) = L(\bar{x}_j, t) \quad (A7)$$

Furthermore, since t only appears in the operator through a derivative then the variable t can be replaced by t_j . Thus

$$L(\bar{x}, t) = L(\bar{x}_j, t_j) \quad (A8)$$

Using Equations (A6) and (A8) then gives

$$L(\bar{x}_j, t_j) \phi_j = 0 \quad (A9)$$

The next task is to determine suitable boundary conditions. Let

$$\begin{aligned}
\phi_j(\bar{x}_U, t_j) &= g_U(\bar{x}_U, t_j) && \text{on } D_{Uj} \\
\phi_j(\bar{x}_D, t_j) &= g_D(\bar{x}_D, t_j) && \text{on } D_{Dj} \\
\phi_j(\bar{x}_u, t) &= 0 && \text{on } D_{Uk}, \quad k \neq j \\
\phi_j(\bar{x}_D, t_j) &= 0 && \text{on } D_{Dk}, \quad k \neq j
\end{aligned} \tag{A10}$$

$$\begin{aligned}
v_j(\pm \bar{x}_j, t_j) &= y'_s(\pm \bar{x}_j, t_j) && \text{on } S_j \\
v_j[\pm(\bar{x}_j - \bar{x}_k), t_j] &= 0 && \text{on } S_{j+k} \quad k = 1, N-1 \\
v_j[\pm(\bar{x}_j + \bar{x}_\ell), t_j] &= 0 && \text{on } S_{j-\ell} \quad \ell = 1, N-1 \\
\Delta C_{pj}(\bar{x}_j, t_j) &= 0 && \text{on } w_j
\end{aligned} \tag{A11}$$

where

$$C_p(\bar{x}, t) = \sum_{-N}^N C_{pj}(\bar{x}_j, t) \tag{A12}$$

It should be noted that in the (x_j, t_j) coordinate system each of elementary problems for ϕ_j is identical.

Periodicity is applied in the $J = \pm N$ blades and their wakes. The wake boundary condition is given by

$$\begin{aligned}
\Delta C_{pj} |(\bar{x}_j - \bar{x}_k), t_j| &= 0 && \text{on } w_{j+k} \quad k = 1, N-1 \\
\Delta C_{pj} |(\bar{x}_j + \bar{x}_\ell), t_j| &= 0 && \text{on } w_{j-\ell} \quad \ell = 1, N-1
\end{aligned} \tag{A13}$$

This is equivalent to keeping all blades stationary except the j th blade and allows the relevant wave transmission through each blade wake. Note that the time is always t_j ,

the time associated with the j th blade. No interblade phase lag is required at this stage.

When ϕ_j are summed, together with the boundary conditions, the problem defined by Equations (A5), (A10), (A11), (A12), and (A13) is identical to the problem defined by Equations (A1), (A2), (A3), and (A4). Hence the problem for any time lag t_0 between blades can be constructed from the superposition of the elementary problem defined by Equations (A9), (A11), (A12), and (A13). The superposition mechanism is as follows.

Let the solution to the elementary problem for $j = 0$ be given by $\phi_0(\bar{x}, t)$. The solution for $\phi_j(\bar{x}, t_j)$ is then given by

$$\phi_j(\bar{x}_j, t_j) = \phi_0(\bar{x}, t) \quad (\text{A14})$$

Since the functional form of ϕ_0 with both \bar{x} and t is known from the elementary solution for $j = 0$ this reparameterization is trivial. The final solution for the zeroth blade is then given by Equations (A5) and (A14); thus

$$\phi(\bar{x}, t) = \sum_{-N}^N \phi_0(\bar{x} - \bar{x}_j, t - jt_0) \quad (\text{A15})$$

Thus the complete time dependent cascade flow for any interblade phase angle can be constructed by superposition of the elementary problem defined by Equations (A5), (A10), (A11), (A12), and (A13).

If $\phi(\bar{x}, t)$ and its derivatives are continuous a similar relation to Equation (A14) can be constructed for the pressure coefficient $C_p(\bar{x}, t)$. In addition, similar formulae can be derived for the lift and moment coefficients.

The idea discussed above can be extended to discontinuous transonic flows using the method of strained coordinates (ref. 2). Results are discussed in the main text.

CONCLUDING REMARKS

The main contribution to the computation time for an unsteady calculation of cascade flutter in a transonic flow is the need to repeat the calculation for a range of inter-blade phase angles. The present analysis shows how this problem can be eliminated by a judicious choice of elementary solutions.

APPENDIX B

LOW STORAGE COMPUTATION OF THE ELEMENTARY SOLUTIONS

In Appendix A it has been shown how an oscillatory flow or an indicial response can be constructed from the superposition of elementary solutions. These elementary solutions consist of one blade moving with other blade held stationary and it becomes clear that the computational storage necessary to retain the information for all the blades in the cascade can be considerable. In this Appendix a suggestion for computing the elementary solution from a computation of the flow between three blades is outlined. Because of the reduced number of blades the computer storage requirements are reduced.

In Appendix A the solution $\phi(\bar{x}, t)$ is given in terms of the elementary solution $\phi_o(\bar{x}, t)$ by

$$\bar{\phi}(\bar{x}, t) = \sum_{j=-N}^N \phi_o(\bar{x} - \tilde{x}_j, t - jt_o) \quad (B1)$$

where t_o is the interblade phase lag and \tilde{x}_j is a spatial shift vector relating the location of the j th blade to the axis.

Now if the interblade phase lag is zero then all the blades are moving in sequence and blade-to-blade periodicity exists. Hence a computation of the cascade requires only three blades with periodic boundary conditions. If such a solution is known, then

$$\phi(\bar{x}, t) = \sum_{j=-N}^N \phi_o(\bar{x} - \tilde{x}_j, t) \quad (B2)$$

Assume now for simplicity that the cascade is unstaggered, then $\tilde{x}_j \equiv y_j$. If the elementary solution throughout the cascade can be represented by some series in the normal variable, y , say then

$$\phi_0(\bar{x}, t) = \sum_{p=0}^{\infty} A_p(x, t) f_p(y) \quad (B3)$$

where the vector \bar{x} has been decomposed into its axial and normal components (x, y) , respectively. $A_p(x, t)$ is an unknown coefficient at x at time t and the $f_p(y)$ are an appropriate orthogonal set of functions representing the variation of $\phi_0(\bar{x}, t)$ with y throughout the cascade. Substitution of Equation (B3) into Equation (B2) gives

$$\phi(\bar{x}, t) = \sum_{j=-N}^N \sum_{p=0}^P A_p(x, t) f_p(y - y_j) \quad (B4)$$

If, in the interval between the three blades, $\phi(x, t)$ is known at P stations in the y -directions then Equation (B4) gives equations for the P unknowns, A_p . Once the A_p are known then the elementary solution can be constructed using Equation (B3). The total solution for any interblade phase lag, t_0 , can then be constructed using the ideas in Appendix A.

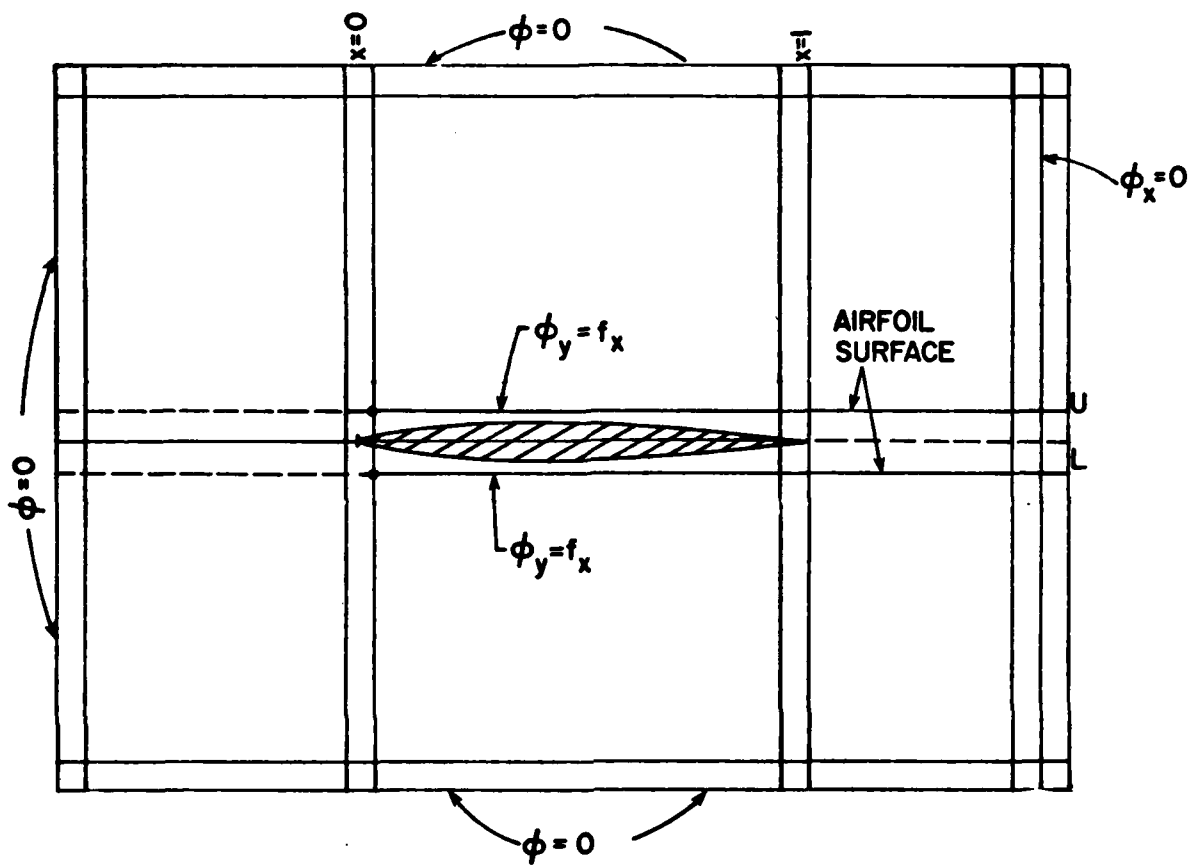


Figure 1. LTRAN2 mesh schematic and boundary conditions for an isolated airfoil.

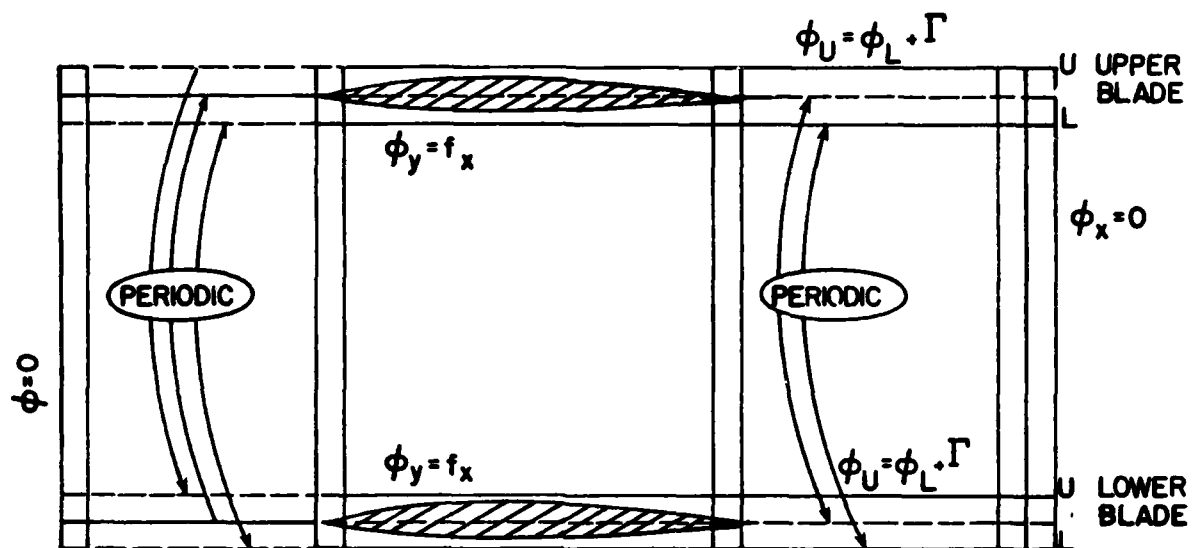


Figure 2. Cascade mesh schematic and boundary conditions for steady state, single blade period. Mesh is clustered near blades, stretched fore and aft.

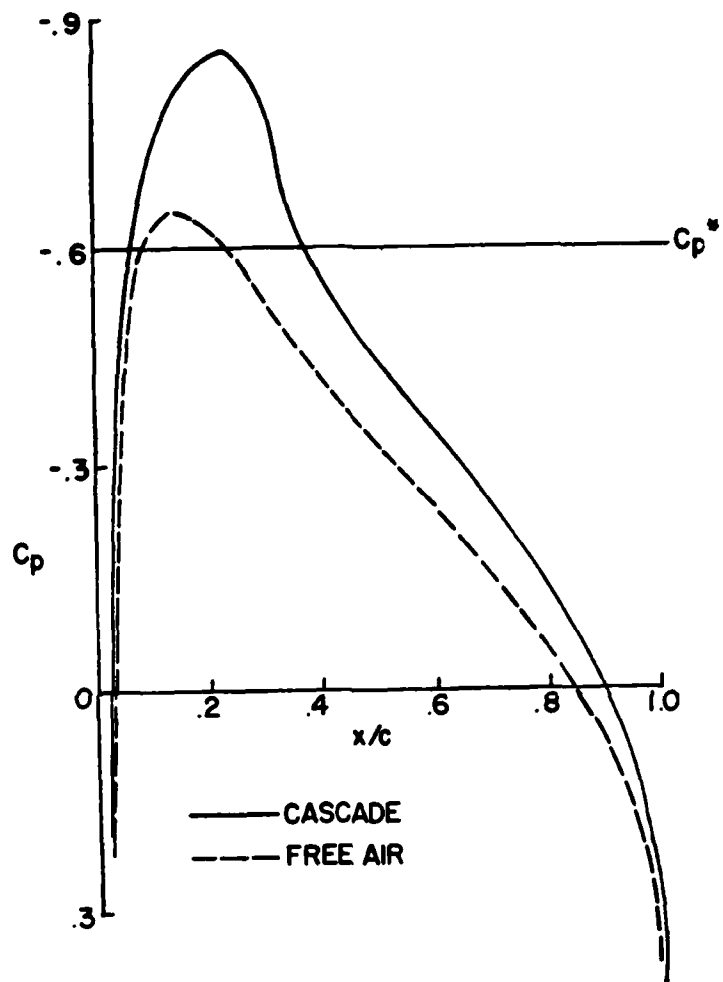


Figure 3. Steady pressure distribution at $M_\infty = .75$ for NACA 0012 airfoil, free air vs. periodic (cascade) boundary condition.

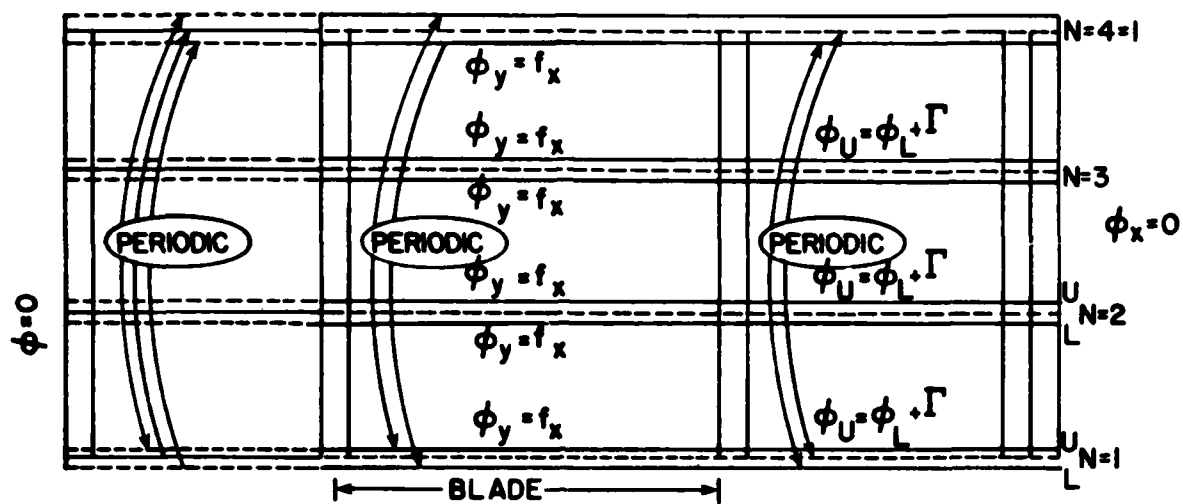


Figure 4. Cascade mesh schematic and boundary conditions for unsteady iterations, illustrated for a 3-blade cascade.

NACA 0012 CASCADE
BLADE #3 INDICIAL RESPONSE

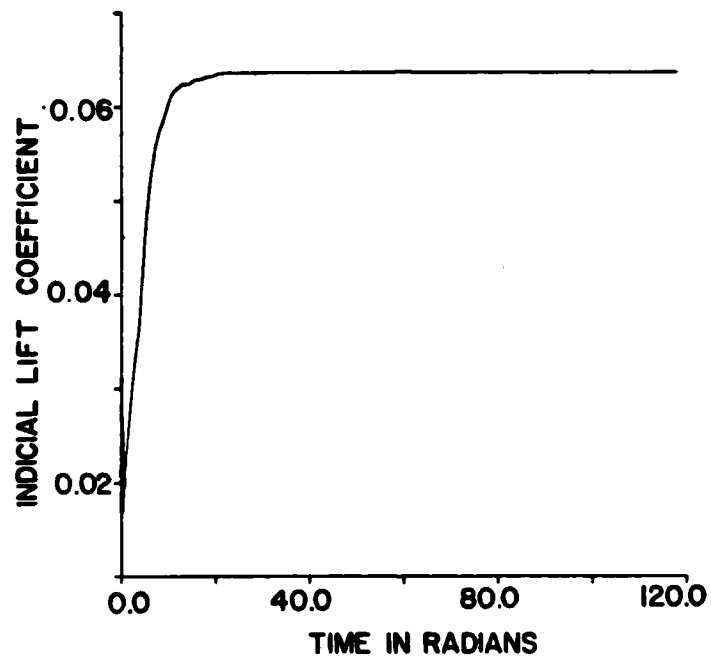


Figure 5. Plot of indicial lift vs. time for blade no. 3 of a 5-blade cascade.

NACA 0012 CASCADE
LOW FREQUENCY OSCILLATION $k=0.2$

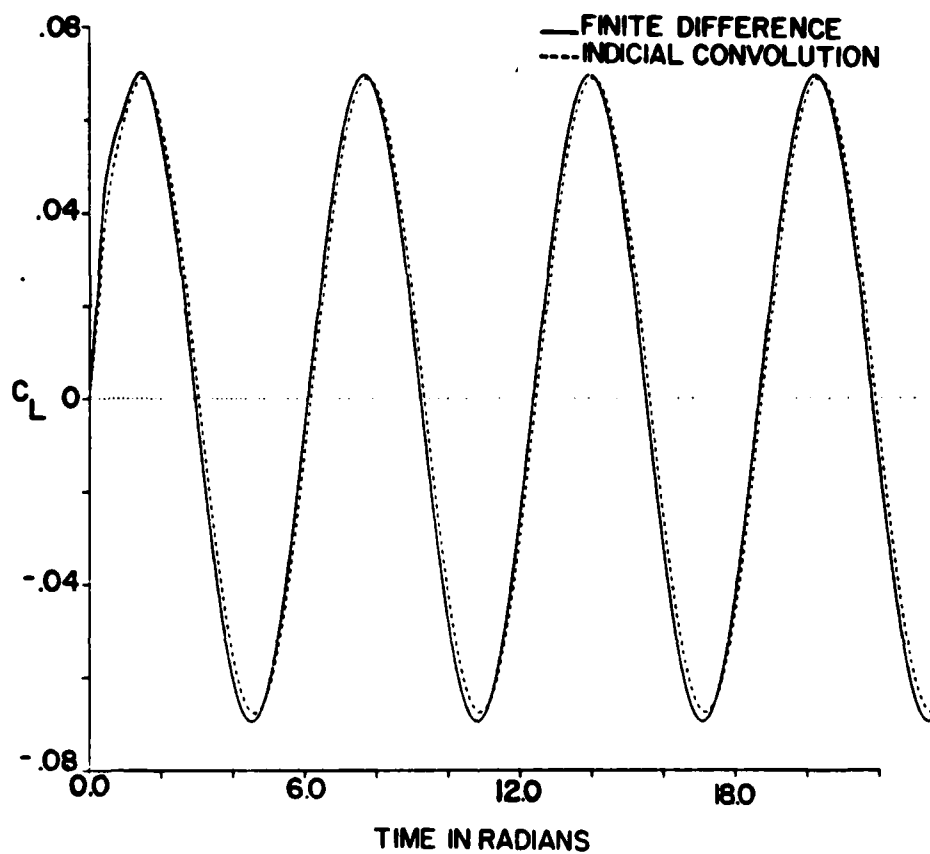


Figure 6. Comparison of finite difference and indicial calculations of oscillatory lift coefficient, $k = 0.2$.

NACA 0012 CASCADE
HIGH FREQUENCY OSCILLATION $k=10.0$

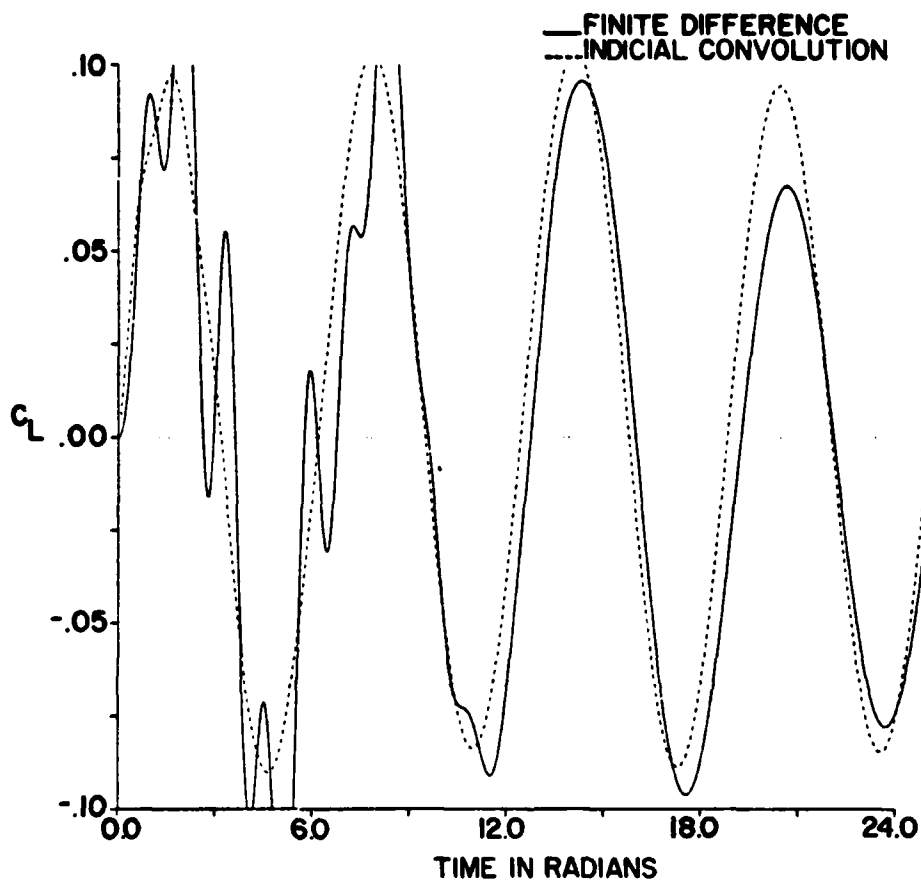


Figure 7. Comparison of finite difference and indicial calculations of oscillatory lift coefficient, $k = 10.0$.

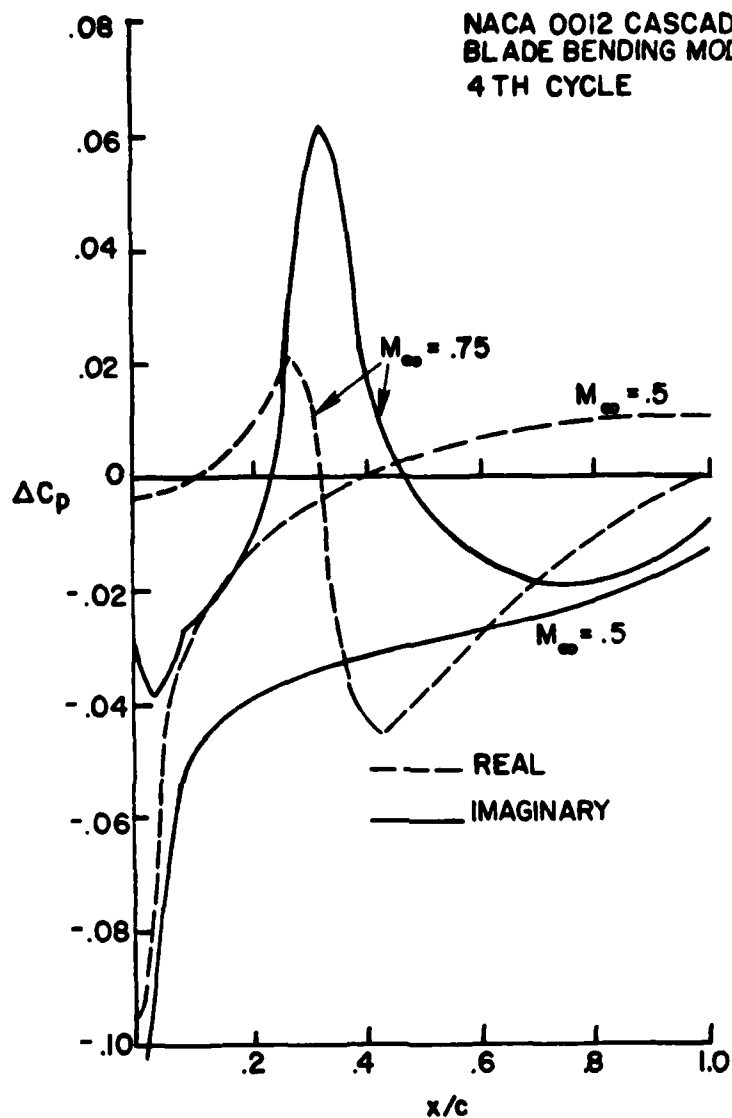


Figure 8. Plot of unsteady pressure difference, 4th cycle, 1st harmonic, for blade #4 bending mode, 6-blade unstaggered cascade of NACA 00012 airfoils. Phase lag is 180 deg. (compare Verdon and Caspar, Fig. 8).

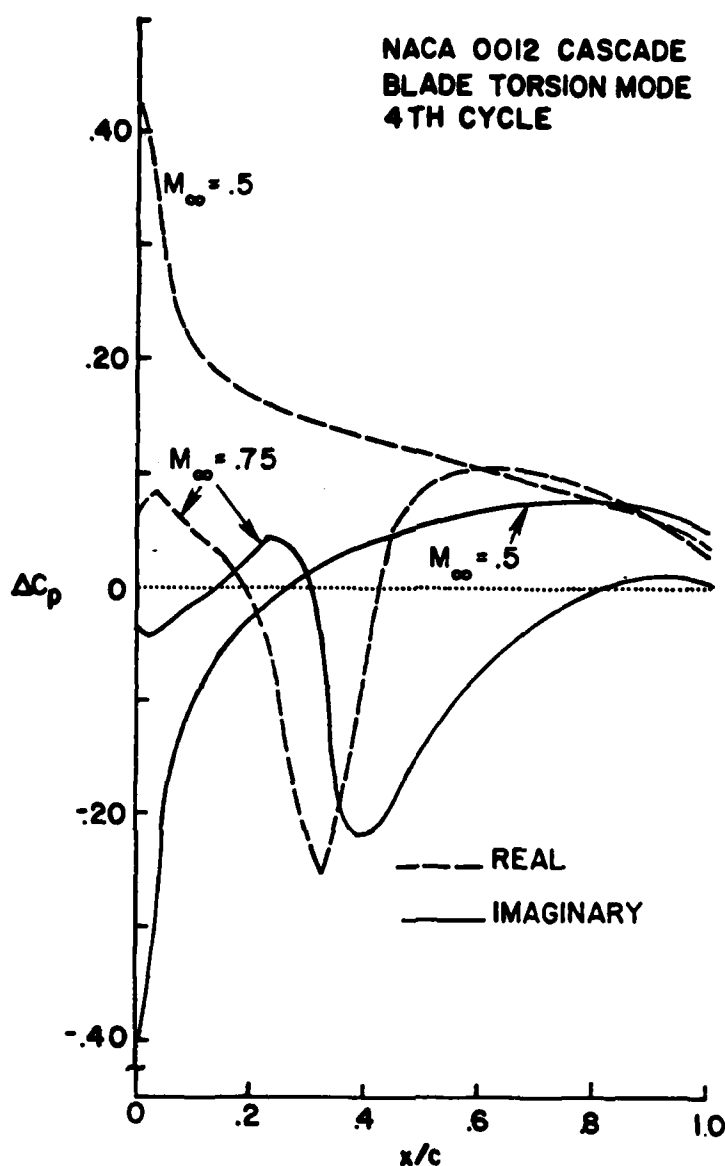


Figure 9. Plot of unsteady pressure difference, 4th cycle, 1st harmonic, for blade #4 torsional mode, 6-blade unstaggered cascade of NACA 00012 airfoils. Phase lag is 180 deg. (compare Verdon and Caspar, Fig. 9)

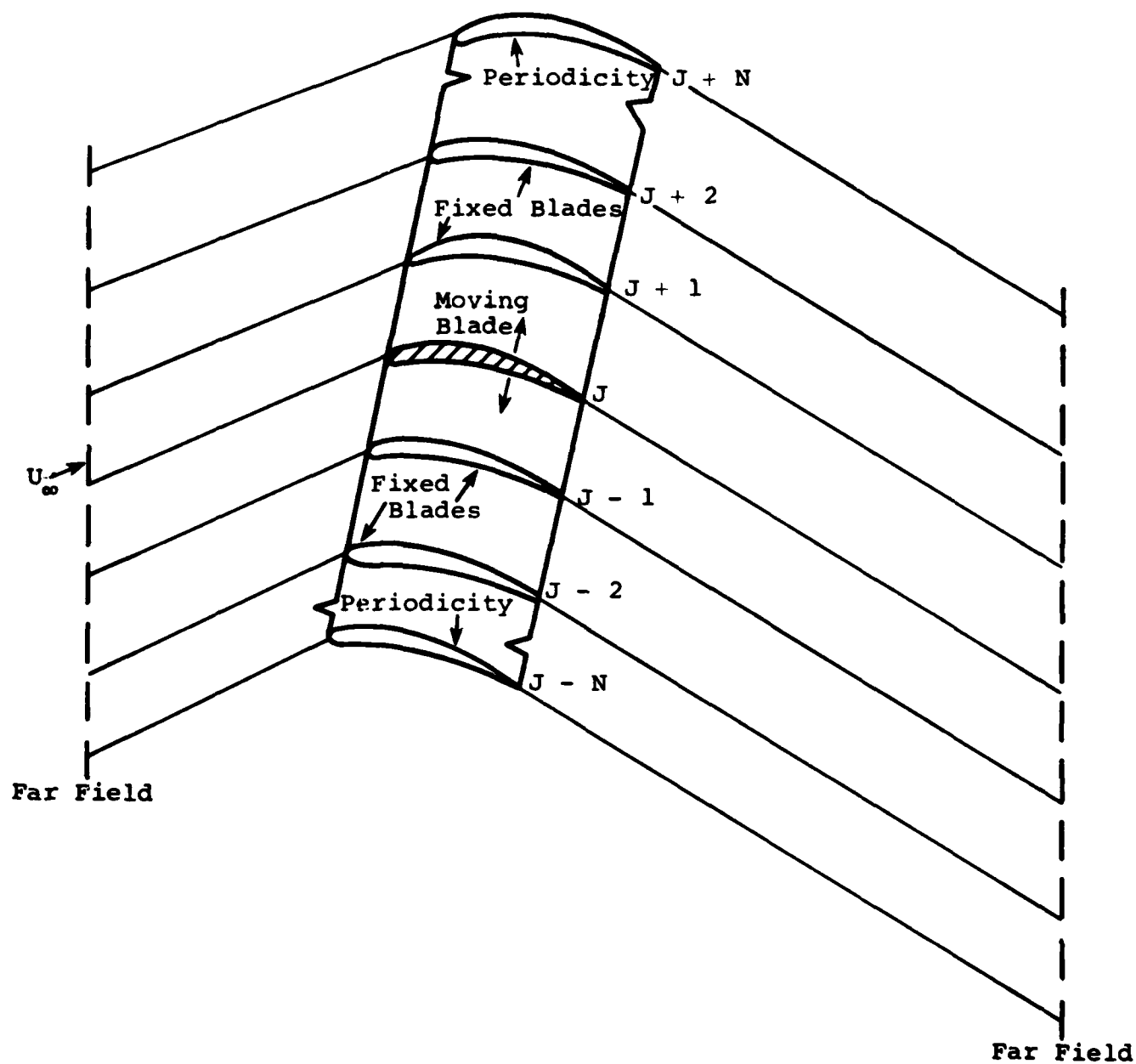


Figure 10. Sketch of Cascade problem.

REFERENCES

1. Lane, F.: System Mode Shapes in the Flutter of Compressor Blade Rows. *Journal of the Aeronautical Sciences*, Vol. 23, No. 1, pp. 54-66, January 1956.
2. Nixon, D.: Notes on the Transonic Indicial Method. *AIAA Journal*, Vol. 16, No. 6, pp. 613-616, June 1978.
3. Ballhaus, W. F. and Goorjian, P. M.: Computation of Unsteady Transonic Flows by the Indicial Method. *AIAA Journal*, Vol. 16, No. 2, pp. 117-124, February 1978.
4. Ballhaus, W. F. and Goorjian, P. M.: Implicit Finite-Difference Computation of Unsteady Transonic Flows about Airfoils. *AIAA Journal*, Vol. 15, No. 12, pp. 1728-1735, December 1977.
5. Houwink, R. and van der Vooren, J.: Results of an Improved Version of LTRAN2 for Computing Unsteady Airloads on Airfoils Oscillating in Transonic Flow. *AIAA Paper 79-1553*, AIAA 12th Fluid and Plasma Dynamics Conference, Williamsburg, VA, July 23-25, 1979.
6. Hessenius, K. A. and Goorjian, P. M.: A Validation of LTRAN2 with High Frequency Extensions by Comparisons with Experimental Measurements of Unsteady Transonic Flows. *NASA TM-81307*, July 1981.
7. Rizzetta, D. P. and Chin, W. C.: Effect of Frequency in Unsteady Transonic Flow. *AIAA Journal*, Vol. 17, No. 7, pp. 779-781, July 1979.
8. Courant, R. and Hilbert, D.: *Methods of Mathematical Physics*. Vol. II, Wiley-Interscience, New York, pp. 511-515, 1962.
9. Kerlick, G. D. and Nixon, D.: Calculation of Unsteady Transonic Pressure Distributions by the Indicial Method. *Journal of Applied Mechanics*, Vol. 49, No. 2, pp. 273-278, June 1982.
10. Verdon, J. M. and Caspar, J. R.: Development of an Unsteady Aerodynamic Analysis for Finite-Deflection Subsonic Cascades. *NASA CR-3455*, September 1981.

END

FILMED

1-83

DTIC